Journal of Thermodynamics & Catalysis

Dhar et al., J Thermodyn Catal 2014, 5:2
DOI: 10.4172/2157-7544.1000134

Research Article Open Access

Thermal Degradation Kinetics of Poly (3-hydroxybutyrate)/Cellulose Nanocrystals based Nanobiocomposite

Prodyut Dhar, Sai Phani Kumar Vangala, Pankaj Tiwari, Amit Kumar and Vimal Katiyar*

Department of Chemical Engineering, Indian Institute of Technology Guwahati, Assam, India

Abstract

Polyhydroxybutyrate (PHB)/ Cellulose nanocrystals (CNCs) nanobiocomposites are prepared by solvent exchange cum solution casting technique at various loading fractions. The effects of CNC loading on dispersion in polymer matrix are studied. Acid hydrolysis of cellulose pulp from bamboo (Bambusabalcooa) yields crystalline rod shaped CNCs having width in the range of 10-20 nm and length being 300-400 nm. Morphological and X-ray diffraction (XRD) studies revealed improved interfacial adhesion of PHB with hydroxyl groups on CNC surface at a threshold loading of 3 wt%. Thermogravimetric analysis (TGA) showed that thermal stability of the nanobiocomposites (PHB/CNC) slightly improved at 3 wt% CNC loading compared to pristine PHB. Further, kinetic analysis of the PHB/CNC nanobiocomposites at different loadings are investigated using isoconversional methods to predict the kinetic triplet. Kinetic parameters predicted from isoconversional methods using Ozawa Flynn Wall (OFW) and Kissinger Akahira Sunose (KAS) models showed that activation energy does not significantly vary with the degree of degradation, revealing that overall degradation follows a single step mechanism. The predicted activation energy values from both OFW and KAS models are in the range of 100-130 kJ/mol The activation energy values are high at higher CNC loadings, showing enhancement in thermal degradation rate due to agglomeration of CNCs. Thermal degradation phenomenon is further studied using Coats Redfern method considering phase boundary controlled models, first order reaction model and power law model. Overall investigation and comparison of the kinetic parameters led to the conclusion that thermal degradation mechanism of PHB/CNC nanobiocomposites followed phase boundary controlled first order reaction models (contracting volume) with random chain scission mechanism.

Keywords: Nanobiocomposite; Polymers; Thermal properties; Cellulose nanocrystals

Introduction

Recent technological advancements and development of novel synthesis processes for fabrication of biodegradable polymers have attracted polymer industries worldwide as a commodity of their interest. These biodegradable polymers have shown potential to substitute conventional petroleum based polymers at industrial scale. Due to their biodegradable and environmental-friendly nature, the use of these biodegradable polymers reduces carbon foot print which subsequently leads to improvement in ecological balance. Biodegradable polymers are usually classified as biopolymers or bio-based polymers depending on their source of origin. The properties of biodegradable polymers need to be critically tailored using different nanofillers and blending techniques to enhance their market applications. Till date several biodegradable polymers have been produced; however, only a few are manufactured at industrial scale such as poly (lactic acid) (PLA) chemically derived from lactic acid precursor, microbially synthesized poly (3-hydroxy butyrate) (PHB), poly (ε-caprolactone) (PCL) from petroleum feedstocks, etc [1,2].

Polyhydroxybutyrate (PHB) is a biodegradable thermoplastic polyester from the family of polyhydroxyalkanoates (PHAs), usually produced from cheap renewable resources by fermentation technique using various microorganisms. However, higher production cost, lower productivity, brittle characteristics and lower thermal stability at processing temperature have limited the wide end applications [3]. Recent studies on incorporation of the nanofillers, usually at lower fractions (1 to 5 wt. %) have shown drastic improvement in the barrier, thermal and mechanical properties of composites compared to pristine polymers [4]. As per literature reports, most widely used nanofillers are nanoclays, metallic nanoparticles, carbon nanotubes etc. The surface characteristics of nanofillers are chemically modified to obtain better dispersion into the polymer matrix. But incorporation of such fillers disturbs the overall biodegradation cycle of biopolymers and problems related to leaching of nanoparticles are observed. Hence, a shift in trend of using non-toxic bionanofillers derived from plant and marine based natural polymers such as cellulose, starch, silk, chitosan etc. have shown improvement in properties while maintaining the biodegradation integrity [5,6]. Biopolymer "cellulose" is abundantly available in the form of lignocellulosic biomass and could be employed as a filler to synthetic biodegradable polymers. Cellulose in its crystalline form usually exist in 20-400 nm range and acts as strong reinforcement agent in polymer through the formation of percolation network due to the strong inter molecular hydrogen bonding [7,8]. Cellulose nanocrystals (CNCs) possess several favorable properties such as nanoscale dimension, high aspect ratio, high specific strength and modulus, high surface area, unique optical properties, etc. [9-11]. These properties make CNC a promising reinforcement nanomaterial with potential application in nanocomposite films, drug delivery, protein immobilization and metallic reaction template.

In present work, hydrophilic CNCs at different loading fractions have been dispersed into hydrophobic PHB through solvent exchange cum solution casting process. Studies carried out by Srithep, et al. [12] for the formation of PHB/CNC nanobiocomposite films through

***Corresponding author:** Vimal Katiyar, Department of Chemical Engineering, Indian Institute of Technology Guwahati, Assam, India, Tel: + 91 361 25822; E-mail: vkatiyar@iitg.ac.in

Received July 27, 2014; **Accepted** August 27, 2014; **Published** September 30, 2014

Citation: Dhar P, Vangala SPK, Tiwari P, Kumar A, Katiyar V (2014) Thermal Degradation Kinetics of Poly (3-hydroxybutyrate)/Cellulose Nanocrystals based Nanobiocomposite. J Thermodyn Catal 5: 134. doi: 10.4172/2157-7544.1000134

melt compounding showed drastic degradation in molecular weight of PHB. Here we report a cost effective process for the fabrication PHB/CNC composites, with an aim to obtain uniform dispersion of CNCs in the biopolymer which subsequently leads to improvement in the thermal properties. The thermal degradation kinetics of PHB and its CNC composites have been investigated using thermogravimetric analysis (TGA) at various heating rates. Detailed kinetic analysis of the degradation process has been performed using model based isoconversional methods to predict the kinetic parameters, i.e. pre-exponential factor, A and activation energy, E. Further, the effect of surface charged groups on CNCs, which have a catalyzing effect on the degradation of PHB, is discussed in detail.

Experimental

Pretreatment of cellulose fibers

Bamboo pulp, supplied by Nagaon Paper Mill, Hindustan Paper Corporation Limited, India has been used as cellulosic biomass source. Pretreatment of the bamboo fibers to remove hemicellulose and lignin content using sodium hydroxide, hydrogen peroxide, (Merck, India) and sodium hypochlorite (Biochem Processing Lab, India) is carried out as per the methodology reported in literature [13].

Synthesis of CNCs

Extracted cellulose from bamboo pulp (1.0 g) is hydrolyzed with 64 wt% sulfuric acid (Merck, India) under vigorous mechanical stirring for 2 hrs at room temperature. Chilled deionized water (Millipore) at 5°C is added to stop the reaction and the suspension is dilute by 10 folds. Further, the suspension is centrifuged and washed with water (several times) to attain pH in the range of 3-4. Homogenization of CNC suspension using IKA-Homogenizer-24 is carried out at ~20000 rpm for 2 min in two cycles. Subsequently, the suspension is dialysed against distilled water to remove excess acid using cellulose acetate dialysis membrane with ~14,000 Da molecular weight cut off (Sigma Aldrich, India). The final suspension is freeze dried to obtain dried powdered cellulose nanocrystals.

Fabrication of PHB/CNC nanocomposites

CNCs have been dispersed into PHB at various loadings through solvent exchange cum solution casting technique which led to improved dispersion without altering the polymer properties. Poly (3-hydroxybutyrate) (purchased from Sigma Aldrich, India) under reflux conditions is dissolved in chloroform at 90°C for 2 hrs. CNCs are solvent exchanged in chloroform through sequential solvent exchange process from water to acetone by centrifugation (10000 rpm) at each step. The uniformly dispersed CNC suspension in chloroform is finally added to PHB melt solution under strong mechanical stirring at 60°C for 20 min. PHB/CNC films at different loadings (1-5 wt%) are solution casted on Teflon plates and dried in fume hood under ambient conditions.

Characterization methods

Wide angle X-ray diffraction (XRD), (Bruker D8 advance, Germany) equipped with Cu Kα generator (λ=0.154 nm) as X-ray source , operating (40 kV, 40 mA) at a scan rate of 0.05° per 0.5 s and scattering intensity measured 2° from 1° to 40° is used to examine the crystal structure of the PHB/CNC nanocomposites. Thermogravimetric Analysis (TGA) (Netzsch) for nanocomposites (~5 mg) is performed under nitrogen atmosphere (at flow rate of 250 mL/min) from 25°C to 500°C at different heating rates. Morphology studies of PHB/CNC nanocomposites and CNC are carried out using field emission scanning electron microscope (FESEM) (Sigma, Zeiss) and atomic force microscopy (AFM) (Agilent, Model 5500 series). WSxM 5.0 Develop 6.5 software (Nanotec Electronica S.L.) has been used for processing the AFM images. For calculation of diameter of CNCs an arbitrary area (consisting of a dense CNC region) is selected on AFM micrograph and corresponding 3D image is generated and average height profile calculated. However, the average length distribution of CNCs is calculated from the AFM topography image.

Kinetic modeling of TGA data: theoretical background

Different kinetic models are proposed to understand the polymer degradation mechanism through prediction of the kinetic parameters based on the data obtained from TGA curves [14].

The kinetic parameters (i.e., A, n and E) can be calculated from TGA data by using the basic rate equation:

$$d\alpha/dt=k(T)\, f(\alpha) \quad (1)$$

where α represents the extent of reaction, which is determined from the TGA data (fractional mass loss), t is time, k(T) represents the temperature dependent rate constant expressed by an Arrhenius type expression and f(α) denotes the particular reaction model, which determines the dependence of the reaction rate on the extent of reaction.

The temperature dependence of the rate constant can be expressed by Arrhenius equation

$$k=A \exp((-E)/RT) \quad (2)$$

where A and E are pre-exponential factor and activation energy, respectively.

Equation (1) can be written as

$$d\alpha/dt= A \exp((-E)/RT)f(\alpha) \quad (3)$$

In order to determine the kinetic triplet (A, E and f(α)), various methods have been developed. They are classified as isoconversional and model fitting methods. In this study two isoconversional models (i.e. Ozawa Flynn Wall and Kissinger Akahira Sunose) and two model fitting methods (i.e. Kissinger and Coats-Redfern) are considered for determining the kinetics of thermal degradation and thermal stability of pristine PHB and PHB/CNC nanocomposites.

Ozawa Flynn Wall (OFW) Model

OFW model is an integral isoconversional method derived by using Doyle's approximation using multiple heating rates TGA data [15]. The model expression is given by

$$\text{Log } \beta=\log AE/g(\alpha)R-2.315-0.4567\, E/RT \quad (4)$$

The plot of log β vs. 1/T gives a straight line whose slope is equal to −0.4567E/RT from which activation energy can be calculated. Pre-exponential factor is calculated from the intercept of the resulting straight line by assuming a reaction model.

Kissinger akahira sunose (KAS) model

KAS is an isoconversional model based on the numerical approximations of the Arrhenius integral over a wide range of thermal history [14]. The model expression is written as

$$\ln(\beta/T\text{^}2)=\ln(AR/(Eg(\alpha)))- E/RT \quad (5)$$

Plot of ln (β/T^2) vs. 1/T yields a straight line. The values of E and A can be calculated from slope and intercept for a particular reaction model.

Kissinger model (KGR)

This is a maximum rate method and applicable only to the multiple heating rate TGA or DTG data [16]. The temperatures (Tm or Tp) at which the rates reach maximum are used to predict the single values of E and A. The expression for this model is

$$\ln\ (\beta/\ T\_p\ ^2)=-(E/(RT\_p)\ )+\ln\ (AR/E) \quad (6)$$

Coats-Redfern model

This method is most widely used for analysis of single heating rate TGA data. The equation for this method is

$$\ln\ (g(\alpha)/T^2\ )=\ln\ [(AR/\beta E)(1-(2RT\ )/E)]-\ E/RT \quad (7)$$

Various solid state reaction models have been reported by several authors previously [17]. Insertion of various expressions shown in Table 1 for g(α) yields different set of E and A values.

Results and Discussions

PHB/CNC composite: morphology and crystalline structure

Hydrolysis of cellulose extracted from the pretreated bamboo pulp with sulphuric acid yields defect free CNCs of typical dimensions ranging from 300-400 nm in length and 10-20 nm in width, with an average aspect ratio ~30. Figure 1a and b illustrate the AFM images of the fabricated CNCs and their corresponding height profile for a selected region (as shown with blue line). The height pattern shows that the diameter of the fabricated CNCs varied within a range of 10-20 nm.

The CNCs are hydrophilic nanoparticles, and hence tend to agglomerate when directly dispersed into hydrophobic polymers such as PHB. Therefore, solvent exchange of freeze dried CNCs is carried out from the easily dispersible solvent water to chloroform in which PHB is readily soluble. This process led to the formation of the stable dispersion of the CNC solution in chloroform, which is also supported from the zeta potential values.

The solvent exchanged CNCs are dispersed into PHB at various loadings and fabricated into films, whose transparency and morphology are studied in detail. CNC loadings above 2 wt% show agglomerations due to poor dispersion and could be detected by visual examination as small white dots on the films. It has been further supported from the transparency values which drastically decreased from 58% to 49%, as the loading was increased to 2 wt%.

Morphological behavior of PHB/CNC nanobiocomposites is further studied by FESEM to understand dispersion and interaction of CNCs with PHB. Two types of orientation of rod like CNCs are found in PHB matrix from thorough investigation of the micrographs. In the first type, CNCs are vertically embedded into PHB matrix, which are seen as white dots/circles, giving the cross sectional view of CNCs. In the second type, CNCs are randomly aligned on the PHB surface. Figure 2a, shows homogenous dispersion of CNCs (at 1 wt% loading) on smooth polymer surface, where majority of nanofillers are embedded into polymer surface, providing more contact area of adhesion. This suggests better adhesion between hydrophilic CNCs and hydrophobic polymer. However, at higher loading fractions (~5 wt.%) agglomeration of the CNCs is observed as shown in Figure 2b.

XRD patterns for pure PHB film and PHB/CNC nanocomposites at various loadings are studied as shown in Figure 3. XRD studies showed broadening of peak at 13.5° and shift to lower 2θ angles, suggesting possible intercalation of CNCs. The hydrogen bonding interaction between the functional groups on the surface of the nanofiller and

Reaction model	Notation	f(α)	g(α)
First order	F1	(1–α)	– ln(1 – α)
Second order	F2	$(1–α)^2$	$α(1 – α)^{–1}$
Phase boundary controlled (contracting area)	R2	$2(1– α)^{1/2}$	$[1 – (1 – α)^{1/2}]$
Phase boundary controlled (contracting volume)	R3	$3(1–α)^{2/3}$	$[1 – (1 – α)^{1/3}]$
Power law model	P4	$2/3\ α–^{1/2}$	$α^{3/2}$

Table 1: Various reaction model expressions for f(α) and g(α).

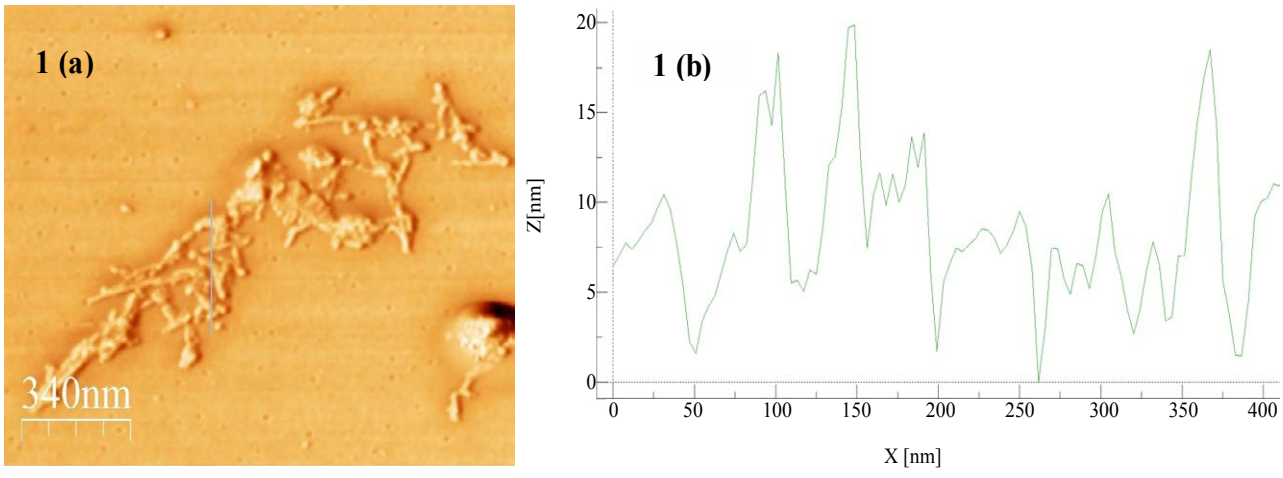

Figure 1: (a) AFM images of the Cellulose Nanocrystals; (b) Height profile of the selected region in AFM image (shown in blue line).

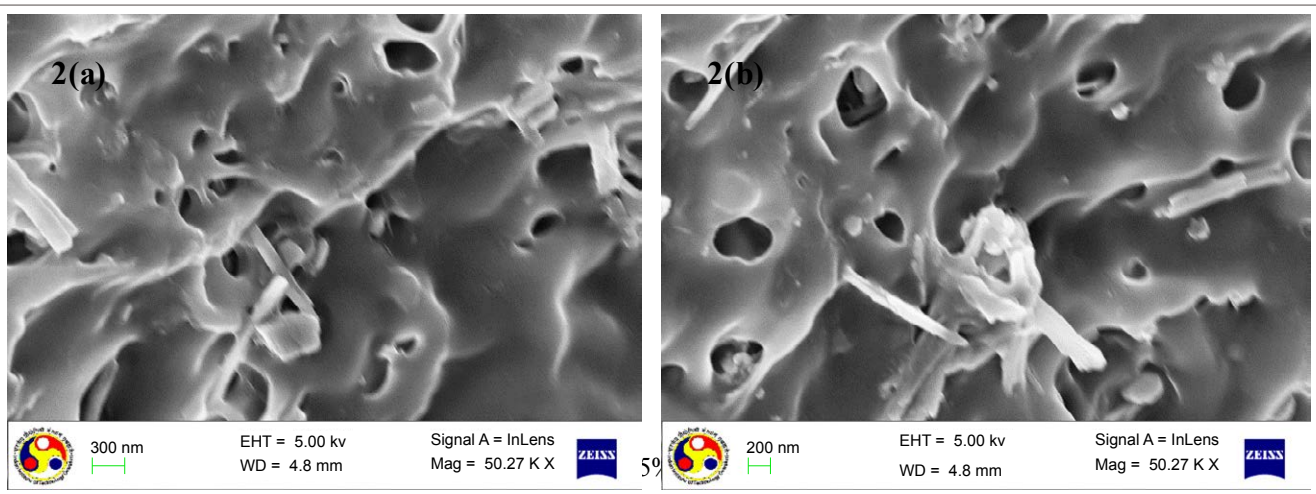

Figure 2: FESEM of PHB film with (a) 1% CNC and (b) 5% CNC.

polymer matrix leads to shifting of the XRD peak at θ=13.5° towards lower angles. The presence of peaks at 2θ=16.5° is a prominent indication of PHB and CNC crystallites in the composites. Moreover, it is found that there is an increase in intensity of cellulose diffraction peaks at 2θ=16.5° and 34.5°, corresponding to (110) and (004) planes on increasing CNCs content to 5 wt%,

PHB/CNC composites: thermal properties

Thermal degradation behavior and thermal stability of pure PHB and PHB/CNC nanocomposites have been determined from single as well as multiple heating rates TGA data shown in Figure 4a and b. It is observed from Figure 4a that the thermal degradation of PHB and its nanocomposites follows the single step mass loss. PHB nanocomposite with 3% CNC loading shows improved thermal stability compared to the pure PHB. However, with increased CNC loadings (~upto 5 wt%), onset degradation temperature decreased from 246°C to 232°C. This shows that CNCs act has a synergistic effect on degradation of the PHB polymer. The enhanced biodegradation might be due to the presence of pendant sulphate and hydroxyl groups on CNC surface which act as nucleation sites for the chain scission of PHB at higher temperature. Thus, biofillers such as CNCs help in enhancing thermal degradation rate of the polymer which is advantageous from environmental point of view. However, rate of degradation (αp) decreases with increase in CNC loadings upto ~3 wt%, reaching a minimum αp value of approximately 24.2 wt%. This is due to the improved compatibility between the PHB/CNCs at lower CNC loadings which led to better hydrogen bonded interaction between nanofiller and polymer subsequently suppressing the polymer degradation rate. However, αp increases at higher CNC loadings (~5wt. %) and the nanocomposite behaves as neat PHB. It could be due to the formation of isolated CNC aggregates in PHB. The residual mass at 500 °C increased with CNC loadings.

Figure 4b shows multiple heating rate TGA curves for PHB/CNC (1%) nanocomposite at 5, 10, 15 and 20°C/min. Like pristine PHB, PHB/CNC (1%) nanocomposite also follows the same degradation behavior with single stage mass loss. The onset (start and end) degradation temperatures increase with increasing heating rate for nanocomposites. Similar TGA curves are obtained for PHB/CNC (5%) nanocomposite at various heating rates.

Estimation of effective activation energy

Evaluation of kinetic parameters from isoconversional kinetic models requires the data obtained from multiple heating rate TGA experiments. Thermal degradation of most of the thermoplastic aliphatic polyesters occurs via random chain scission mechanism. Likewise PHB also degrades by random chain scission via β-elimination of crotonic acid and crotonoate oligomers [18]. First order reaction model is considered in KAS and OFW models for the determination of kinetic parameters using multiple heating rates data. Figure 5a and b shows the plot of log β vs. 1/T from OFW model for (a) PHB/CNC (1%) and (b) PHB/CNC (5%) nanocomposites at various extents of conversions with four linear intervals of heating rates. The resulting straight lines in Figure 5a are shifted to left hand side from α = 0.1–0.9 with increase in slope up to α=0.6 and slight decrease for α=0.7 and 0.8. The slopes of the straight lines are gradually reduced from α=0.1–0.9 in case of PHB/CNC (5%) as shown in Figure 5b. Kinetic parameters calculated from OFW model for PHB/CNC (1 and 5%) nanocomposites are tabulated in Table 2.

It is observed from Table 2, that 'E' and 'A' values increased for nanocomposite containing 1% CNC till α=0.6 and then reduced suddenly. The best fit (R2=1) is obtained at α=0.8 but the 'E' and 'A' values are lower. In case of PHB/CNC (5%) nanocomposite, the 'E' and 'A' values changes rapidly with extent of conversion. The change in activation energy and pre-exponential factor values are notable at initial stages of degradation (i.e. α=0.1–0.2 and α=0.3–0.4).

The plots obtained by KAS model for PHB/CNC (1%) and PHB/CNC (5%) nanocomposites at multiple heating rates are shown in Figure 6 a and b respectively. The kinetic parameters calculated from KAS model for PHB/CNC (1 and 5%) nanocomposites are listed in Table 3.

The kinetic parameters (i.e. E and A) calculated from KAS model are in good agreement with the values evaluated from OFW model. The variation of 'E' with extent of conversion indicates that the occurrence of complex reactions involving different mechanisms rather than degradation by simple mechanisms. The 'E' and 'A' values determined from Kissinger model (maximum rate method) are 105.6 kJ/mole and 2.3379×1010 min^{-1} respectively for PHB/CNC (1%) and 108.7 kJ/mole and 1.2927×1011 min^{-1} respectively for PHB/CNC (5%) nanocomposite.

Coats Redfern method is applied to determine kinetic parameters and the mechanism of thermal degradation using several reaction

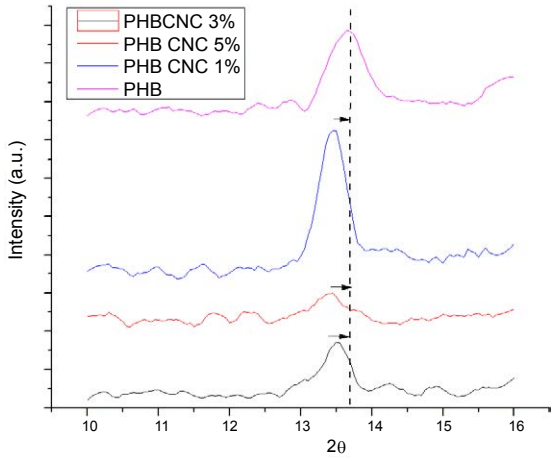

Figure 3: XRD comparison of dspacing and Dhkl of PHB film with different CNC loaded films.

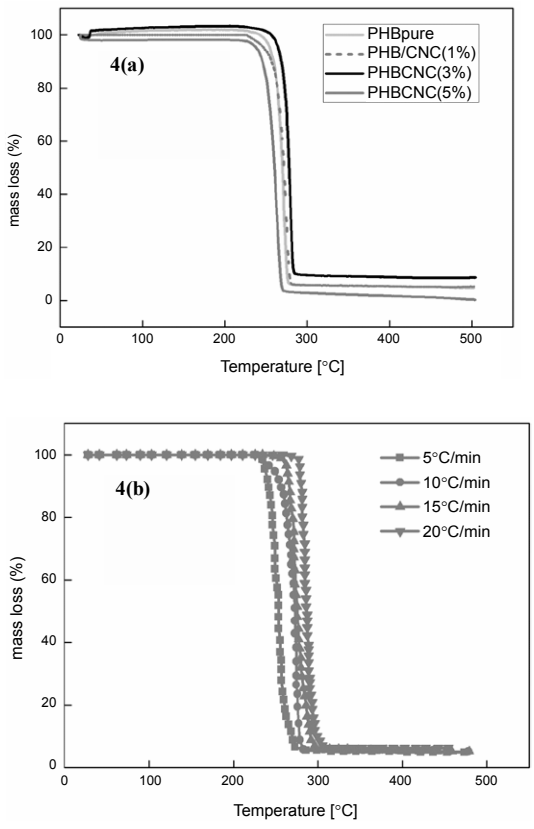

Figure 4: (a) TGA curves of pure PHB and PHB/CNC with various amounts of CNC at 10°C/min. (b) TGA curves of PHB/CNC (1%) nanocomposites at multiple heating rates.

models indicated in Table 4 for single heating rate TGA curves at 10°C/min, as shown in Figure 6. Five reaction models have been used in Coats Redfern method in order to determine the best suitable reaction model which represents the experimental data effectively. Figure 7 shows Coats Redfern plot, ln(g(α)/T^2) vs. 1/T for pure PHB obtained from TGA curve at a heating rate of 1°C/min.

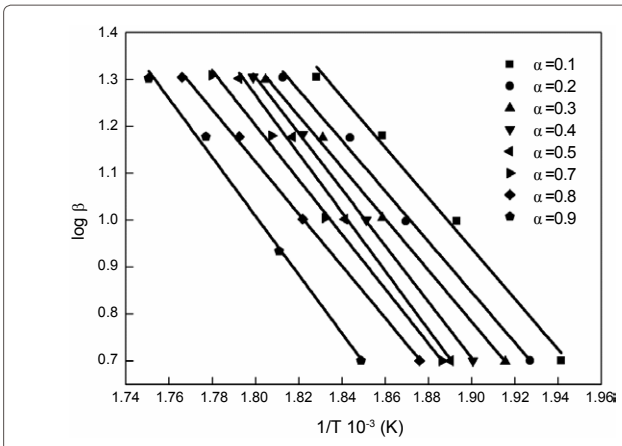

Figure 5: OFW plots of (a) PHB/CNC (1%) and (b) PHBCNC (5%) nanocomposites at different conversions obtained from multiple heating rate TGA curves.

For all five models the trend is same but the slopes and intercepts are different. The 'E' and 'A' values are found from the slope and intercept of each straight line. The values of activation energies evaluated for pristine PHB and for bionanocomposites from the Coats Redfern method are summarized in Table 4.Various reaction models yield different 'E' values. Phase boundary controlled models (i.e. contracting area and contracting volume) yield lower activation energy values while the regression coefficients are high. The 'E' values evaluated from first order reaction are intermediate between second order and phase boundary controlled models. For pure PHB as well as for nanobiocomposites, first order reaction model represents best fits (R2~1). The values of 'E' calculated from second order reaction model are quite high compared to other reaction models. Power law model presents most relevant values of 'E' which are also close to values reported in earlier investigations [18]. Selection of a single model from the different models considered is very difficult and each model has its own limitation. At low and high percentages of CNC, thermal stability of nanobiocomposite is less than the pristine PHB while at 3% of CNC thermal stability is increased due to better interaction between the polymer matrix and the filler and also due to good dispersion of nanofiller. At higher percentages of nanofiller, agglomeration of nanofiller in polymer matrix occurs, which subsequently leads to enhanced degradation. This is revealed by kinetics from isoconversional and model fitting analyses. Overall, thermal degradation of pure PHB and PHB/CNC nanocomposites containing various percentages of nanocomposites follows first order reaction model with random chain scission mechanism and phase boundary controlled reaction models (contracting volume).

Conclusion

Fabricated PHB/CNC nanobiocomposites showed better dispersion at a threshold CNC loading of ~3 wt%, as suggested from the morphological orientation of the CNC in FESEM micrographs. XRD studies showed shift of the PHB peak to lower theta angles, representing improved interaction of the hydrophilic CNCs with hydrophobic PHB. Thermal degradation kinetics study of PHB/CNC nanobiocomposites revealed that thermal stability slightly improved upto CNC loading of ~3 wt%. Isoconversional analysis of thermal properties and evaluation of kinetic parameters using OFW and KAS models didn't show significant change in activation energies. This could be attributed to the degradation mechanism which follows single step degradation and

Extent of conversion (α)	PHB/CNC (1%)			PHB/CNC (5%)		
	E	A	R^2	E	A	R^2
0.1	96.9	2.1385×10^{8}	0.9910	127	6.2565×10^{11}	0.9949
0.2	97.4	4.1162×10^{8}	0.9915	116	6.917×10^{10}	0.9716
0.3	100.8	1.208×10^{9}	0.9831	114.3	5.8834×10^{10}	0.9959
0.4	109.2	1.023×10^{10}	0.9667	103.5	5.839×10^{9}	0.9925
0.5	113.4	3.1451×10^{10}	0.9681	112	4.9713×10^{10}	0.9914
0.6	114	5.1431×10^{10}	0.9785	105.1	1.0919×10^{10}	0.9922
0.7	107	1.3969×10^{10}	0.9906	101.5	5.7666×10^{9}	0.9912
0.8	101	3.5711×10^{9}	1	106.9	2.4427×10^{10}	0.9949
0.9	111.2	3.80×10^{10}	0.9829	103.8	1.4496×10^{10}	0.9928

Table 2: Kinetic parameters with regression coefficients from OFW model for PHB/CNC (1 and 5%) nanocomposites.

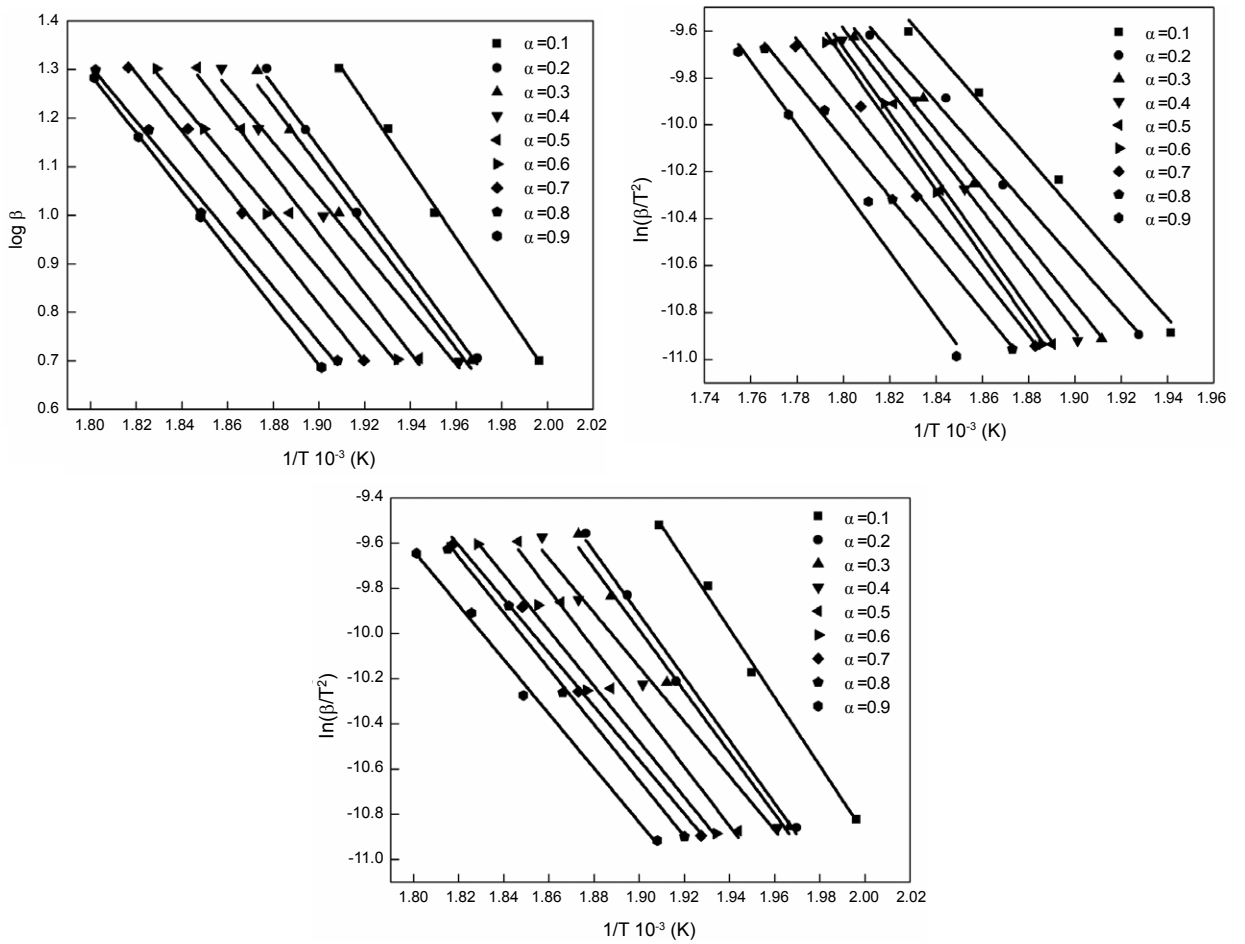

Figure 6: KAS plots of (a) PHB/CNC (1%) and (b) PHB/CNC (5%) nanocomposites at different conversions obtained from multiple heating rate TGA data.

Extent of conversion (α)	PHB/CNC (1%)			PHB/CNC (5%)		
	E	A	R2	E	A	R2
0.1	93.1	6.5025×10^{7}	0.9890	125.2	3.6072×10^{11}	0.9941
0.2	93.6	1.2454×10^{8}	0.9897	115.3	4.1902×10^{10}	0.9825
0.3	101	9.6962×10^{8}	0.9818	111.5	2.6229×10^{10}	0.9953
0.4	105.9	3.8482×10^{9}	0.9610	100.1	2.0946×10^{9}	0.9912
0.5	110.3	1.2687×10^{10}	0.9629	109.2	2.0797×10^{10}	0.99
0.6	118	1.0058×10^{11}	0.9761	101.7	3.9245×10^{9}	0.9908
0.7	104.4	5.0134×10^{9}	0.9889	97.8	1.9049×10^{9}	0.9894
0.8	100.7	2.4592×10^{9}	1	103.5	8.9542×10^{9}	0.9940
0.9	111	2.979×10^{10}	0.9838	100.3	4.9376×10^{9}	0.9915

Table 3: Kinetic parameters with regression coefficients from KAS model for PHB/CNC (1 and 5%) nanocomposites.

Reaction model	PHB pure	PHB/CNC (1%)	PHB/CNC (3%)	PHB/CNC (5%)
	E	E	E	E
First order (F1)	108	83.3	118	83.2
Second order (F2)	152	121	174.6	117.6
Phase boundary controlled (R2)	91	70.2	104	71
Phase boundary controlled (R3)	96.4	74.3	110	76.2
Power Law (P4)	117.6	91.4	133	93.3

Table 4: Activation energy values evaluated from Coats Redfern method using five reaction models for pure PHB and PHB nanocomposites.

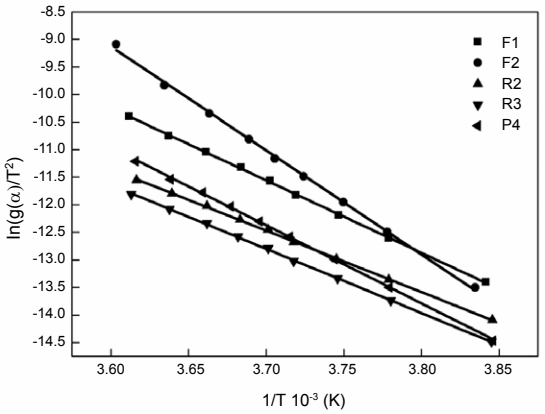

Figure 7: Coats Redfern plots using five reaction models for pure PHB at 10°C/min

remains unchanged for neat PHB and all other nanobiocomposites. On further evaluation of the kinetic parameters with different models, it is concluded that PHB/CNC nanobiocomposites follows first order reaction and phase boundary controlled reaction models (contracting volume) with random chain scission mechanism.

Acknowledgement

Authors would like to express their gratitude to Central Instruments Facilities (CIF) and Department of Chemical and Petrochemical (DCPC, GoI) funded Centre of Excellence for Sustainable Polymers (CoE-SusPol), Indian Institute of Technology, Guwahati, India for providing the research and analytical facilities.

References

1. Chen GQ (2009) A microbial polyhydroxyalkanoates (PHA) based bio- and materials industry. Chem Soc Rev 38: 2434-2446.
2. Lunt J (1998) Large-scale production, properties and commercial applications of polylactic acid polymers. Polym Degrad Stab 59: 145–152.
3. Doi Y, Kanesawa Y, Kunioka M, Saito T (1990) Biodegradation of microbial copolyesters: poly(3-hydroxybutyrate-co-3-hydroxyvalerate) and poly(3-hydroxybutyrate-co-4-hydroxybutyrate). Macromolecules 23: 26–31.
4. Bordes P, Pollet E, Avérous L (2009) Nano-biocomposites: Biodegradable polyester/nanoclay systems. Prog Polym Sci 34: 125–155.
5. Ten E, Turtle J, Bahr D, Jiang L, Wolcott M (2010) Thermal and mechanical properties of poly(3-hydroxybutyrate-co-3-hydroxyvalerate)/cellulose nanowhiskers composites. Polymer 51: 2652–2660.
6. Svagan AJ, Åkesson A, Cárdenas M, Bulut S, Knudsen JC, et al. (2012) Transparent films based on PLA and montmorillonite with tunable oxygen barrier properties. Biomacromolecules 13: 397-405.
7. Umesh Bhardwaj (2013) Evaluation of discrete kinetics during pyrolysis of lignocellulosic biomass and its extracted pulp (ENFL606).
8. Wu D, Wu L, Wu L, Zhang M (2006) Rheology and thermal stability of polylactide/clay nanocomposites. Polym. Degrad Stab 91: 3149–3155.
9. Habibi Y, Lucia LA, Rojas OJ (2010) Cellulose nanocrystals: chemistry, self-assembly, and applications. Chem Rev 110: 3479-3500.
10. Ten E, Bahr DF, Li B, Jiang L, Wolcott MP (2012) Effects of Cellulose Nanowhiskers on Mechanical, Dielectric, and Rheological Properties of Poly(3-hydroxybutyrate-co-3-hydroxyvalerate)/Cellulose Nanowhisker Composites. Ind Eng Chem Res 51: 2941–2951.
11. Xu X, Liu F, Jiang L, Zhu JY, Haagenson D, Wiesenborn DP (2013) Cellulose Nanocrystals vs. Cellulose Nanofibrils: A Comparative Study on Their Microstructures and Effects as Polymer Reinforcing Agents. ACS Appl Mater Interfaces 5: 2999–3009.
12. Srithep Y, Ellingham T, Peng J, Sabo R, Clemons C, Turng LS, et al. (2013) Melt compounding of poly (3-hydroxybutyrate-co-3-hydroxyvalerate)/nanofibrillated cellulose nanocomposites. Polym Degrad Stab 98: 1439–1449.
13. Yu M, Yang R, Huang L, Cao X, Yang F, et al. (2012) Preparation and characterization of bamboo nanocrystalline cellulose. BioResources 7: 1802–1812.
14. Vyazovkin S, Sbirrazzuoli N (2006) Isoconversional Kinetic Analysis of Thermally Stimulated Processes in Polymers. Macromol Rapid Commun 27: 1515–1532.
15. Carrasco F, Pérez-Maqueda LA, Sánchez-Jiménez PE, Perejón A, Santana OO, et al. (2013) Enhanced general analytical equation for the kinetics of the thermal degradation of poly(lactic acid) driven by random scission. Polym Test 32: 937–945.
16. Cho YS, Shim MJ, Kim SW (1998) Thermal degradation kinetics of PE by the Kissinger equation. Mater Chem Phys 52: 94–97.
17. Ebrahimi-Kahrizsangi R, Abbasi MH (2008) Evaluation of reliability of Coats-Redfern method for kinetic analysis of non-isothermal TGA. Trans Nonferrous Met Soc China 18: 217–221.
18. Ariffin H, Nishida H, Shirai Y, Hassan MA (2008) Determination of multiple thermal degradation mechanisms of poly(3-hydroxybutyrate). Polym Degrad Stab 93:1433–1439.